UNCLASSIFIED

Defense Technical Information Center
Compilation Part Notice

ADP012463

TITLE: Comparison Between the M256 120-MM Tank Cannon Jump Test Experiments and ARL's Gun Dynamics Simulation Codes for Prototype KE

DISTRIBUTION: Approved for public release, distribution unlimited

This paper is part of the following report:

TITLE: 10th U.S. Army Gun Dynamics Symposium Proceedings

To order the complete compilation report, use: ADA404787

The component part is provided here to allow users access to individually authored sections of proceedings, annals, symposia, etc. However, the component should be considered within the context of the overall compilation report and not as a stand-alone technical report.

The following component part numbers comprise the compilation report:
ADP012452 thru ADP012488

UNCLASSIFIED

COMPARISON BETWEEN THE M256 120-MM TANK CANNON JUMP TEST EXPERIMENTS AND ARL'S GUN DYNAMICS SIMULATION CODES FOR PROTOTYPE KE

J. F. Newill,[1] B. J. Guidos,[1] and C. D. Livecchia[2]

[1] *U.S. Army Research Laboratory, AMSRL-WM-BC, Aberdeen Proving Ground, MD 21005*
[2] *U.S. Army Armament Research Development and Engineering Center,* AMSTA-AR-FSF-T, *Picatinny Arsenal, NJ 07806*

The interaction between the gun system and projectile cannot be directly measured during the launch event, leaving the interaction to be inferred from the exit state conditions of the projectile through various recording devices. The only direct means of studying the in-bore motion of the projectile and projectile-gun system interaction is through numerical simulation. The best approach for validation of the Army Research Laboratory's (ARL) gun-projectile dynamic simulation codes is comparison with projectile motion data obtained from ARL ballistic jump test experiments. In such tests, four or more sets of orthogonal radiograph images (x-rays) are typically used to characterize the state of the projectile at muzzle exit. The results from the x-rays can be directly compared to the predictions made by the gun-projectile dynamic simulations. This paper describes the methodology used to compare recent jump test data to gun-projectile dynamic simulations and presents comparisons for seven 120-mm prototype kinetic (KE) energy projectiles. The projectiles contain significant differences in their charge, subprojectile, and sabot designs that span the design parameters encountered in cartridge development.

Improving accuracy for both direct- and indirect-fire weapons is a major challenge to the ballistician during gun and projectile development. The ability to control the interior and exterior ballistic processes to minimize adverse dynamic perturbations to the projectile during the launch represents a major step toward "designing in" accuracy. Recently, emphasis has been placed on the direct-fire accuracy of tank main armament systems to enhance the lethality of this class of weapon and to improve accuracy of supersonic kinetic energy (KE) projectiles. Fundamental understanding of gun system and projectile interaction is paramount to meeting this goal. In addition to the direct effects launch has on accuracy, the interior ballistic motion sets the dynamic state of the projectile during the transitional and exterior ballistics phases of flight to a target. Experimentally, the interaction between the gun system and projectile cannot be determined during the launch event, leaving the interaction to be inferred from the exit state conditions of the projectile through various recording devices. The only direct means of studying the in-bore motion of the project and projectile-gun system interaction is through numerical simulation. The best approach for validation of the U.S. Army Research Laboratory's (ARL) gun-projectile dynamic simulation codes is comparison with projectile motion data obtained from ARL ballistic jump test experiments.

1. JUMP MODEL

The complete set of jump test data provides a range of information concerning the launch and flight behavior of the rounds. A substantial portion of the data is used to construct a jump diagram for each shot. The jump diagrams are based upon a jump closure model that characterizes the launch and flight aspects of the rounds, as well as providing a basis for statistical analysis of the entire set of rounds. The jump model has been presented along with the techniques in reports by Bornstein et al. (1988), Bornstein et al. (1989); and Plostins et al. (1990) and is briefly reviewed here.

The total jump of a particular shot can be defined as the vector angle between projectile target impact and the pre-trigger line of fire, with gravity drop removed. The jump vector is defined using the nomenclature introduced in Figure 1.

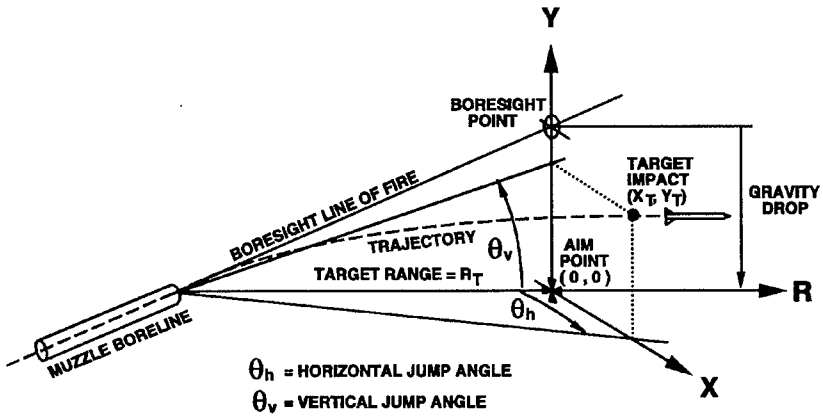

FIGURE 1. ILLUSTRATION OF JUMP ANGLES.

The boresight line of fire is established as the line connecting the center of the muzzle and boresight point obtained by the muzzle borescope. The gravity drop can be extracted separately from various data sources, including the radar track, and is considered known. The line of fire and gravity drop together establish a target aim point from which the target impact point is measured. The resulting vector is denoted as (X_T, Y_T), with the subscript "T" representing the values at the target impact point. For the KE projectiles of interest here, the magnitude of this vector is small enough compared to the target range, R_T, such that the vector is converted directly into an angle, in radians, when divided by the range to form the total jump, $\overline{\theta}$, (small angle assumption), i.e.,

$$\overline{\theta} = \theta_h \hat{i} + \theta_v \hat{j} \cong {}^{X_T}\!/_{R_T}\, \hat{i} + {}^{Y_T}\!/_{R_T}\, \hat{j} \qquad (1)$$

In the above expression, θ_h and θ_v are the horizontal and vertical components, respectively, of the total jump. The unit vector $\hat{i}$ is oriented to the gunner's right (positive X in Figure 1) and the unit vector $\hat{j}$ is oriented up (positive Y in Figure 1), and these orientations represent jump coordinates as used in this paper.

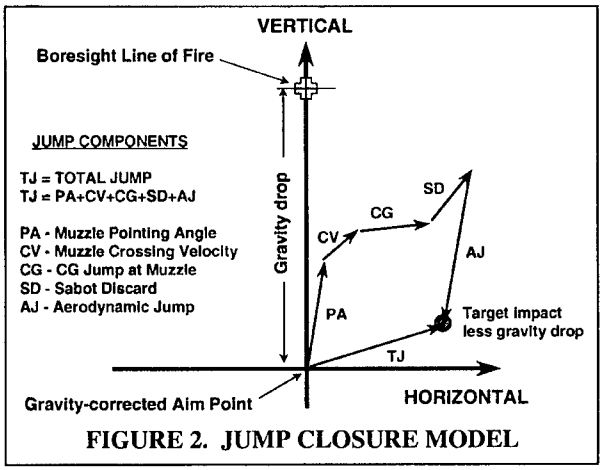

FIGURE 2. JUMP CLOSURE MODEL

The jump closure model, shown in Figure 2, follows that which has been presented in previous jump tests (Bornstein et al. 1988; Plostins et al. 1990). The origin is defined as the intersection of the horizontal and vertical axes (labeled H and V) and represents the aim point. The aim point is determined by subtracting the gravity drop from the boresight line of fire. The target impact point is denoted as a solid circle. A set of five vectors is defined whose summation is equal to the vector whose tail is located at the aim point and whose head is located at the target impact point. These vectors are jump component vectors, each having a horizontal and vertical component, and are defined as follows:

Muzzle Pointing Angle (*PA*) - The muzzle pointing angle at the time of shot exit relative to the aim point.

Muzzle Crossing Velocity Jump (*CV*) - The angular deviation corresponding to muzzle lateral motion, obtained by dividing the muzzle lateral velocity at shot exit by the projectile launch velocity.

Center-of-Gravity Jump (*CG*) - The angular deviation of the subprojectile center of gravity (c.g.) at the muzzle relative to the instantaneous bore centerline at shot exit. Also referred to in previous jump tests as the jump due to mechanical disengagement of the projectile from the gun tube. The vector arises from the c.g. motion caused by the balloting interaction between the projectile and the gun tube.

Sabot Discard Jump (*SD*) - The angular deviation of the projectile c.g. attributable to the transverse disturbance arising from the sabot discard process.

Aerodynamic Jump (*AJ*) - The angular deviation of the projectile c.g. attributable to aerodynamic lift forces associated with the free-flight projectile yawing motion. The source of the angular deviation is the angular rate at muzzle exit combined with the angular impulse caused by sabot discard.

In addition, the Total Center-of-Gravity Jump (CG_{TOT}) is defined as the sum of the *PA*, *CV*, and *CG* jump vectors. The CG_{TOT} jump represents the angular deviation of the center-of-gravity at muzzle exit, relative to the pre-trigger line-of-fire.

2. INSTRUMENTATION AND TEST APPARATUS

Figure 4 is an illustration of the primary instrumentation situated around the tank and the line of fire. The measurement techniques follow the general set up and procedures described in reports of previous tests conducted at Aberdeen Proving Ground (APG) (Schmidt et al. 1984; Bornstein et al. 1988; Plostins et al. 1990). Table 1 lists the approximate ranges of the instrumentation.

A muzzle pressure probe, used to provide an electronic trigger to the various recording devices, is positioned a few centimeters from the muzzle and supported by a cantilever that rotates away from the muzzle when impacted by the initial blast. Four sets of orthogonal x-ray stations are situated at four non-overlapping axial stations within 10 m from the muzzle, Figure 3.

Each station consists of a pair of orthogonal 150 kV flash x-ray units and associated film with screen intensifiers enclosed and protected in wooden cartridge cases constructed prior to the test. The x-ray units are mounted onto a steel x-ray rig, shown in Figure 2, and the loaded cartridges secured onto the rig prior to each shot.

TABLE 1 DISTANCES FOR INSTRUMENTATION POSITIONS AS MEASURED FROM MUZZLE.

Instrumentation	Range (m)
Eddy Probe Station #1	-0.495
Eddy Probe Station #2	-0.343
X-Ray #1	0.5
X-Ray #2	2.5
X-Ray #3	4.5
X-Ray #4	7.5
Orthogonal Smear Camera	10
High Speed Video Camera	30
Yaw Cards #1	37
Yaw Cards #2 thru #15	7.0 m spacing
Yaw Card #16	142
Target	963

A set of eight proximity gauges (eddy probes) are mounted onto a specially constructed self-supporting aluminum rig slid over the gun tube to a location approximately 50 cm from the muzzle, as shown in Figure 5. The eddy probe rig is designed to secure two groups of four eddy probes each at two axial locations approximately 15 cm apart. Each eddy probe returns a voltage signal that corresponds to the distance between the probe tip and the gun. Prior to each shot, the eddy probes are adjusted within the rig to be positioned approximately 0.04 inches from the tube surface, where a highly linear voltage

signal exists. A temporary sunscreen, visible in Figure 3, is constructed from wood, cloth, and rope to shield the gun tube from direct sunlight and to minimize gun tube movement induced by disparate heating (Bundy et al. 1993).

FIGURE 3. X-RAY RIG.

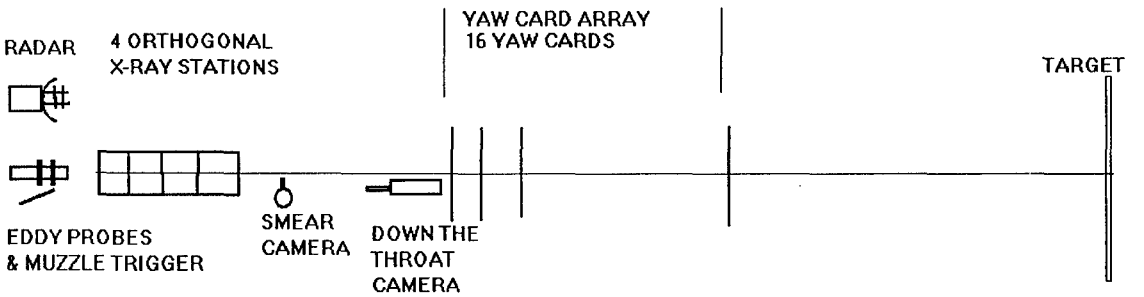

FIGURE 4. INSTRUMENTATION SET-UP

The complete set of eddy probe data is reduced in the post-test analysis into the form of muzzle pointing angle and lateral displacement as a functions of time using the procedure reported by Bornstein and Haug (1988). From this data, the *PA* and *CV* jump vector components can be obtained as part of the jump analysis. This data could also be used to compare with numerical simulations if the muzzle motion itself was simulated and stored during the numerical procedure. However, such is not the case for the numerical simulation approach used here, where projectile motion parameters, rather than muzzle motion parameters, are compared.

The jump test setup also consists of yaw card stations equally spaced along the line of fire at axial locations between 37 and 142 m forward of the muzzle. The cloth target is located 963 m downrange of the muzzle. Two orthogonal color smear camera images are collected at 10 m from the muzzle. The smear images are obtained by exposing highly sensitive film that is spooled at a high rate of speed as the projectile passes through the image domain. A "down-the-throat" high-speed video camera records each launch event using a line of sight acquired by a mirror positioned 30 m from the muzzle and approximately 0.6 m below the line of fire. Weibel radar data is collected for each firing. With accompanying electronics and equipment, the instrumentation provided the data and visual records necessary to calculate the set of jump components sought for the particular shot.

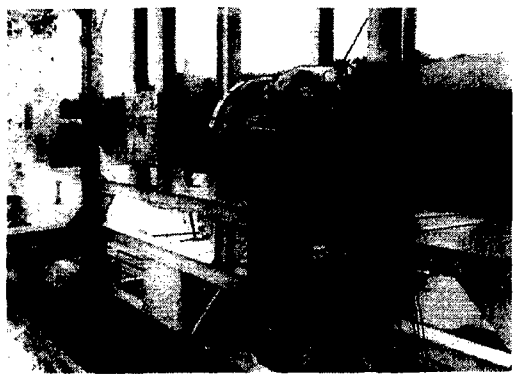

FIGURE 5. EDDY PROBE RIG.

The general test procedure for each shot is as follows: The muzzle is aimed at a pre-determined point on the target using a collimated borescope. This boresight point, typically the lower right corner of the square formed by the intersection of the horizontal and vertical cross, is then surveyed. The cardboard yaw cards are mounted to the wooden support frames and marked with horizontal and vertical reference lines using the boresight. The loaded x-ray cassettes are secured into the rig. A fiducial cable is a steel cable containing two reference beads at each x-ray station is hung along the line of fire, as shown in Figure 6.

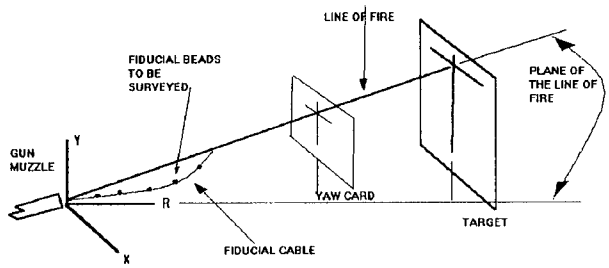

FIGURE 6. TEST SET-UP

The steel fiducial cable is supported at the downrange end of the rig by a laterally adjustable pulley sighted to be near the line of fire, and at the breech by a metal plate. Mass of approximately 60 kg is hung from the downrange end of the cable, reducing the droop of the cable to a few millimeters. The applied mass forces the metal plate to abut tightly against the breech housing. The plate is laterally adjusted such that the cable is centered at the muzzle. The cable contains fiducial beads at each x-ray station to provide orientation and magnification references. Survey is conducted of the cable position at the muzzle, the pulley, and the fiducial beads. The x-ray film is exposed at a low power level to mark the bead locations, the cable is removed, and the pulley is lowered via a hinged platform attached to the x-ray rig. The eddy probes are adjusted, all instrumentation is set to initiate at pulse trigger, and firing commences.

3. MEASURED PROJECTILE MUZZLE EXIT STATE AND JUMP COMPONENTS

A single x-ray station is drawn schematically in Figure 7. After the fiducial cable and beads are exposed onto the x-ray film prior to the shot, the shot is fired and x-rays are taken of the projectile in flight. In each x-ray image, the position and orientation of the projectile are measured and can be related to the boresighted line of fire determined from the cable image. Linear fits are made to the projectile lateral position and angular orientation, thus providing measured values of projectile angular and translational rates at muzzle exit. Projectile angular rate and projectile lateral translation rate at muzzle exit are the two quantities that are compared in the validation of numerical

simulation with experimental measurement. The values are extracted from the data at a time that corresponds to shot exit, defined here as the instant in time when the rear bourrelet (also called the rear bore rider or bulkhead) mechanically disengages from the gun tube. At this time, the obturator undergoes a process of disintegration and the main blast uncorks.

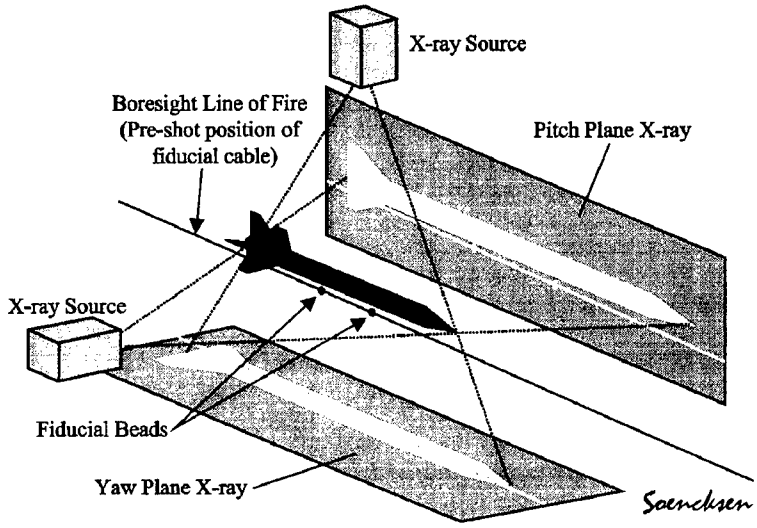

FIGURE 7. ORTHOGONAL X-RAY SETUP.

The CG_{TOT} jump vector is directly related to the lateral translation rate at muzzle exit. The CG_{TOT} jump is obtained by dividing the projectile lateral translation rate (a two component vector, plane transverse to the line of fire) by the projectile launch velocity. The AJ vector is closely related to the projectile angular rate at muzzle exit. Guidos and Cooper (1999) used a linear impulse model to generalize the expression given by Murphy (1963) that relates projectile angular rate at the muzzle and aerodynamic jump. For application to a KE projectile with sabot discard, the expression can be approximated and written in complex coordinates (the transformation between complex coordinates and range coordinates, consistent with that used by Guidos and Cooper (1999) is not an issue of concern here) as:

$$AJ = -k_t^2 \frac{C_{L\alpha}}{C_{M\alpha}} \left(\tilde{\xi}_0' + \tilde{\vartheta}_l^* \right) \tag{3}$$

where, k_t^2 = subprojectile non-dimensional radius of gyration,

$C_{L\alpha}$ = subprojectile aerodynamic lift force coefficient derivative,

$C_{M\alpha}$ = subprojectile aerodynamic pitching moment coefficient derivative,

$\tilde{\xi}_0'$ = subprojectile angular rate at muzzle exit (rad/caliber)

$\tilde{\vartheta}_l^*$ = change in subprojectile angular rate attributable to sabot discard (rad/caliber)

$\tilde{\xi} = \alpha + i\beta$ = subprojectile angle of attack in complex coordinates

α = pitch angle (positive up)

β = yaw angle (positive nose left)

In the above equation, the subprojectile angular rate at muzzle exit, $\tilde{\xi}_0'$, is a measure of the total angular impulse applied to the projectile by the gun. The change in subprojectile angular rate attributable to sabot discard, $\tilde{\vartheta}_l^*$, is a measure of the total angular impulse applied to the

subprojectile during the sabot discard process. Further discussion of the quantity $\tilde{g}_I^*$ is made by Guidos and Cooper (1999).

To complete the discussion of jump components, it is noted that the *SD* jump vector is typically obtained through closure, where the aerodynamic jump vector is placed on the jump diagram such that its tip is coincident with the actual recorded projectile impact point. The *SD* vector is constructed such that closure is achieved between the tip of the *CG* vector and the base of the *AJ* vector, as shown in Figure 2. As stated, this vector is actually a combination of the *SD* vector and the sum of all measurement errors, which are typically on the order of 0.2 mrad or less (Lyon et al, 1991).

4. NUMERICAL SIMULATION OF TANK GUN PROJECTILES

Gun/projectile dynamic simulations utilize three-dimensional (3-D) Finite Element (FE) models of the M256 120-mm tank cannon launching projectiles (Figure 8. The method is described in Rabern 1991; Wilkerson and Hopkins 1994; Burns, Newill, and Wilkerson (1998); Newill, Burns, Wilkerson (1998); Newill et al. (1998a, 1998b, 1998c, 1999a, 1999b, 2000); Guidos et al. (1999). The hydrocode finite element formulation was chosen to allow investigation of stress wave propagation due to elements of launch. The models are 3-D to capture the asymmetric response of the projectile and gun system resulting from the nonlinear path of the projectile during launch, asymmetric boundary conditions, general lack of symmetry in the centerline profiles of the gun tube, and asymmetric gun motion.

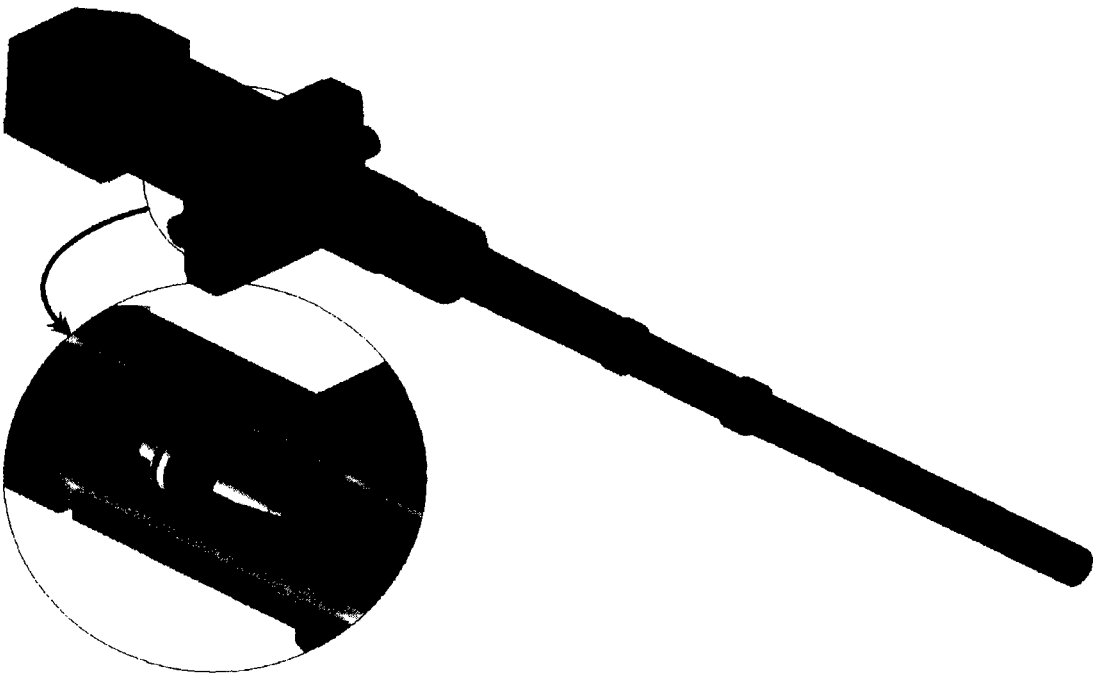

FIGURE 8 M1'S M256 GUN SYSTEM WITH KE PROJECTILE SHOWN IN-BORE.

The projectiles and gun systems are both built in similar manners. Models are developed for the components and then integrated. Relative motion is obtained by defining the proper physics to allow interaction between the parts. Since this projectile is relatively simple, the nose, body, stabilizer and obturator are welded together, and sliding interfaces are defined between the nose, body, stabilizer, between the sabot petals, and the gun bore. One of the purposes of these types of studies, is to estimate tank fleet performance. In order to do this, the projectile model is integrated

into (and fired from) a number of gun models each of which have unique tube centerlines (the centerlines are covered later in this paper). The propellant pressure loading for the gun system and projectile is generated from IBHVG2 (Anderson and Fickie, 1987) which provides good quality interior ballistic prediction for production charges.

The gun dynamic simulation codes predict the transverse rates (velocity and angular rate) during the launch cycle (Figure 9). Three types of information are used from these predictions, the dynamic path, variability in jump, and the average jump. The dynamic path gives qualitative information on the rate history of the projectile during the launch cycle. The variability and average jump predicted by the codes are related to accuracy errors where reduction in variability or error represents improved performance of the system.

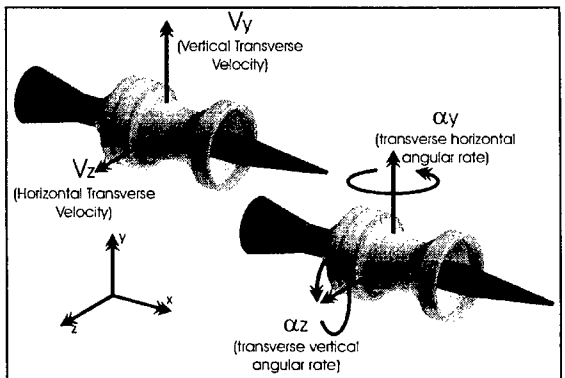

FIGURE 9. DEFINITION OF TRANSVERSE RATES

To intentionally induce the variability into the dynamic path which results in variability the muzzle exit rates, a series of initial conditions are used. The initial condition that has the strongest influence is the initial cocking angle of the projectile in the forcing cone/bore. Since the diameter of the projectile's bourrelets is less than the interior bore and forcing cone diameter, there exists a clearance between the projectile and the gun tube. The angle the centerline of the projectile can make with these confines is defined as the cocking angle. Therefore, the cocking angle is relative to how the gun bore/forcing cone and chamber are manufactured, the projectile and cartridge's manufacturing dimensions along with total run-out of the cartridge (how straight the cartridge is made). There are an infinite number of ways that the projectile can be cocked in tube, but typically, the cocking angles used in simulations are up, down, left, right, and straight since they encompass the maximum variability. The cocking angles are calculated on a model by model basis using the specific dimension of the particular projectile/gun geometry. The straight projectile has the forward and rear bourrelet centered relative to the initial location of the projectile in the gun.

In order to validate the gun codes, some type of methodology is required in order to compare various projectiles performance. Since the phenomena being predicted is nonlinear and stochastic in nature and the initial conditions are not known precisely on a shot-by-shot basis, the gun dynamic codes are used to predict an envelope of performance. This is consistent with the experimental methodology. Typically a series of projectiles shots are simulated to predict both the center of impact (COI) and variability. Essentially, in the gun codes to induce the variability, the initial conditions are varied, typically projectile initial cocking angles up, down, left, right, and straight; then a series of simulations is accomplished (Newill 1998a). Using these simulations, the range of angular rates and range of transverse velocities are predicted.

On a smaller scale, this is consistent with the how the gun codes are used to predict performance. To define projectile "tank fleet" performance the same type of data is predicted, but it is combined with multiple gun systems at a range of temperatures. When comparing to experimental data only one gun tube and propellant temperature combination is used. Figure 10 shows how the envelope predicted from the simulations and measured in the experiment at compared. In Figure 10, there are four items of interest: the experimental data, predictions from the simulation, the envelope (variability) of performance from the simulation, and 95% confidence level for the experimental data. The comparison between the experiment and simulation is made through the relative sizes of the variability and the averages of predicted and measured data.

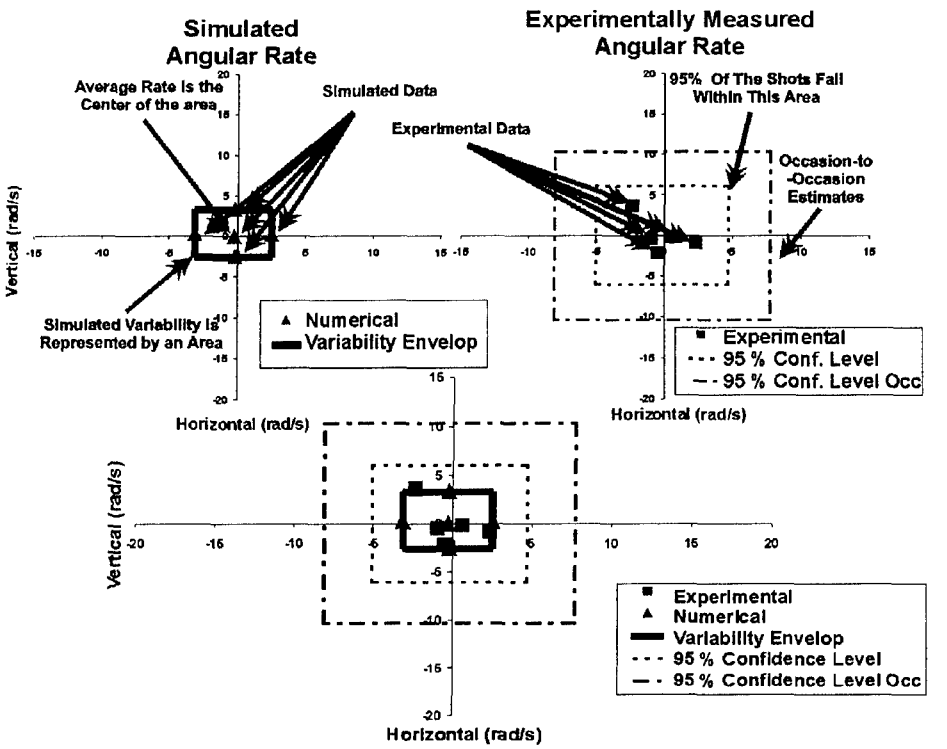

FIGURE 10. SIMULATION COMPARISON WITH EXPERIMENTAL RESULTS.

It is very important to note that the experiment is a ballistic phenomenon that is not entirely predictable. Even with production ammunition, with as many factors as possible controlled, there can be significant deviation of the shooting performance. For this reason, there can never be absolute comparison between the simulated data and the experimental data.

Figure 11 shows an extrapolation of the experimental data to help understand and define the 95 % confidence level and occasion to occasion envelope. The figure uses the experimental data to predict the shot patterns directly from the experiment and using the empirical knockdown factor applied to the experimental results. The figure shows that the two boxes essentially define the two different groups. These two boxes are used to define the performance of the experimental data.

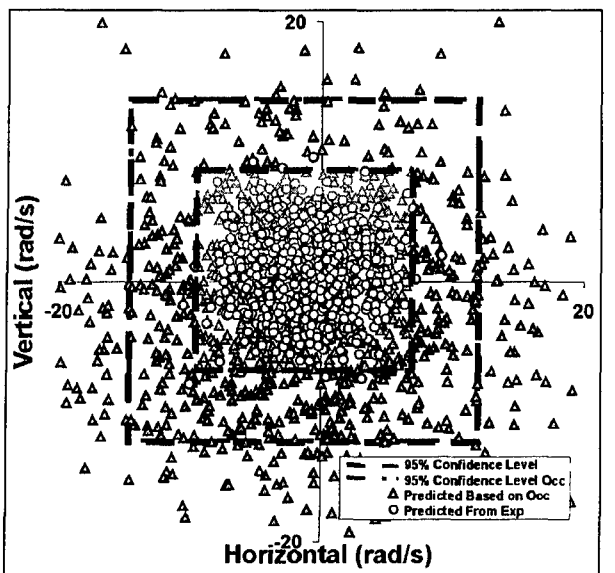

FIGURE 11. EXPLANATION OF THE 95 % ENVELOPE AND OCCASION TO OCCASION ENVELOPE.

The variability predicted should typically be smaller than the variability (95% confidence level) in the experiment, although working with prototype projectiles complicates the situation. Prototype projectiles are made in small numbers with custom-designed propellant charges. Both the small numbers and custom charge induce variability that would not be seen in a well-made production projectile. Other reasons for the variability in the experimental data to be larger than the simulation data is related to ambiguity

in shot start (fracture of the case adapter), variability due to the propellant burning,* and the fracture problem at muzzle exit associated with the breaking of the obturator. Each of these is significant and is attacked through other means as separate problems to reduce variability and improved projectile performance.

There are two ways that the average is compared to the experimental data. The first level compares the simulation data to the experimental data, the average should lie within the 95% confidence level of the experimentally measured values. Unfortunately, due to the nature of tank firing, a second envelope needs to be used. The issue is related to what is typically called occasion-to-occasion error. It basically accounts for differences in the experimental data seen when firing the same tank at two different times while still controlling the other factors of the experiment. The second box represents the uncertainty from this source is determined using empirical methods based on a history of shooting results. The average of the simulation data should lie within the occasion to occasion estimate for a good comparison.

In spite of this ambiguity, the resulting model is quite capable of accomplishing numerical sensitivity studies (given that appropriate computer assets are available). Several ballistic issues have been studied, including the following:

- The effect of projectile initial condition on shot exit kinematics.
- The effect of subtle projectile geometry variations on both shot fall dispersion and mean jump.
- The effect of gun tube centerline profile on both shot fall dispersion and mean jump.
- The comparison of projectile design to assess the accuracy attributes of different designs.
- Studies to ascertain the means to reduce the dynamic motion of the gun barrel.

For many of the projectile modifications accomplished using this tool, the results have been confirmed through large numbers of projectile firings.

5. COMPARISONS BETWEEN EXPERIMENT AND SIMULATION

The predictions from the projectile/gun dynamics simulation codes can be very useful if it can be related to the physical system. In this section, several examples are shown to show the range of comparison between experiment and simulation. The ballistic data was obtained in jump tests conducted by ARL at Army Test Center (ATC).

Seen in Figure 12 through Figure 18, the experimental and simulated data compare well in both variability and average to the experimental data.

Only in the last two figures are the average rates significantly different from the experiments, although the variability data is fine. In Figure 19, the rates of the horizontal and horizontal angular velocity can be seen to be changing rapidly near muzzle exit. The horizontal component is seen to change much faster especially during the last 0.4 ms of travel. Also, if there is a time error in muzzle exit and the projectile actually exited earlier than predicted, then both horizontal components move toward zero, which is what was seen in the experiment. There are several aspects of the simulation that can cause variability in muzzle exit times relative to the experiment. The first is differences in muzzle exit time. While these differences are small in magnitude, it implies that the projectile exited early. Other problems with these predictions have to do with shot start and propellant variability. The shot start has to do with the projectile not moving until the propellant has developed enough pressure to break the case-base adapter. The propellant issue deals with variability due to development of the flame and the symmetry of the burning. In any of these cases, the exit time can vary.

---

* The propellant can burn asymmetrically and generate large transverse pressure waves. Either effect can severely degrade the performance of the projectile or destroy it.

For the projectile design in Figure 20, examining the same quantities shows that the accelerations near muzzle are relatively low and that the change in rates is also very low. In each case, the simulation and experiment show a very good correlation and provides insight into how sensitive the performance is to small changes in muzzle exit time. Figure 21 and Figure 22 show what happens to the experimental/simulation comparisons when these small time differences are considered. Figure 21 clearly shows that the transverse velocity matches well at the earlier time whereas the angular rate data is not affected as much. Figure 22 shows the same type of comparison for a well behaved projectile. Here the comparisons are almost identical regardless of the exact exit time.

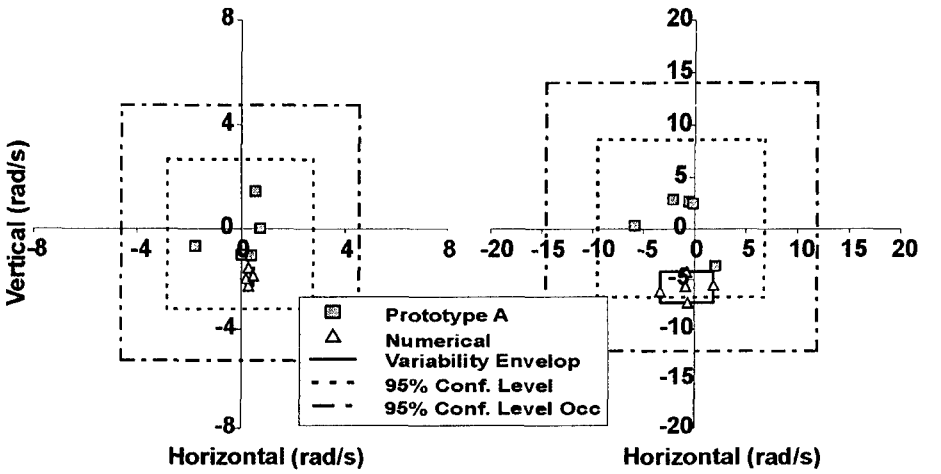

FIGURE 12. TRANSVERSE VELOCITY AND ANGULAR RATE COMPARISONS, RESPECTIVELY FOR PROJECTILE A.

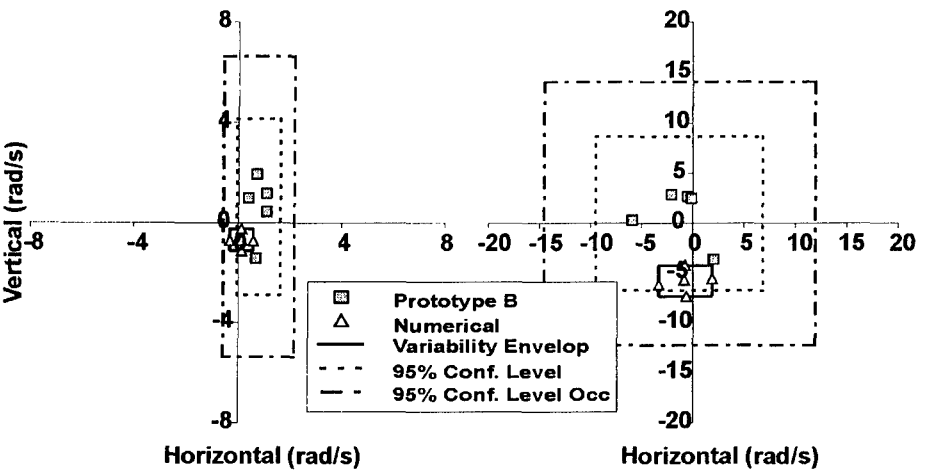

FIGURE 13. TRANSVERSE VELOCITY AND ANGULAR RATE COMPARISONS, RESPECTIVELY FOR PROJECTILE B.

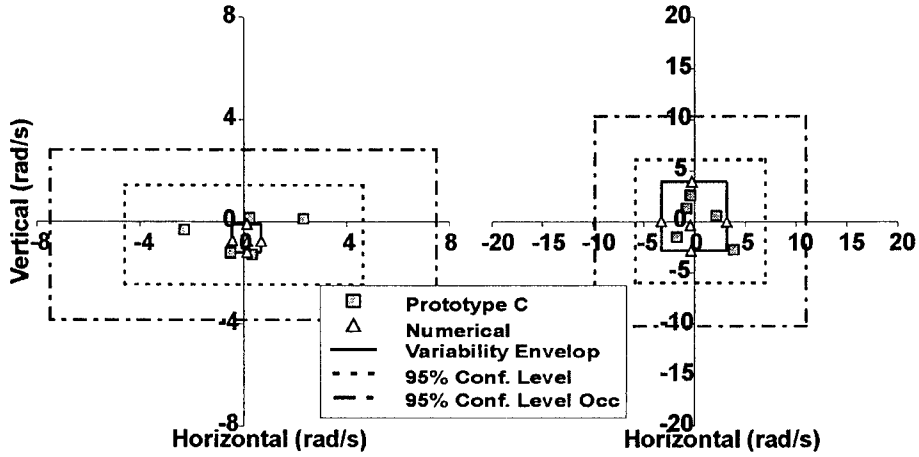

FIGURE 14. TRANSVERSE VELOCITY AND ANGULAR RATE COMPARISONS, RESPECTIVELY FOR PROJECTILE C.

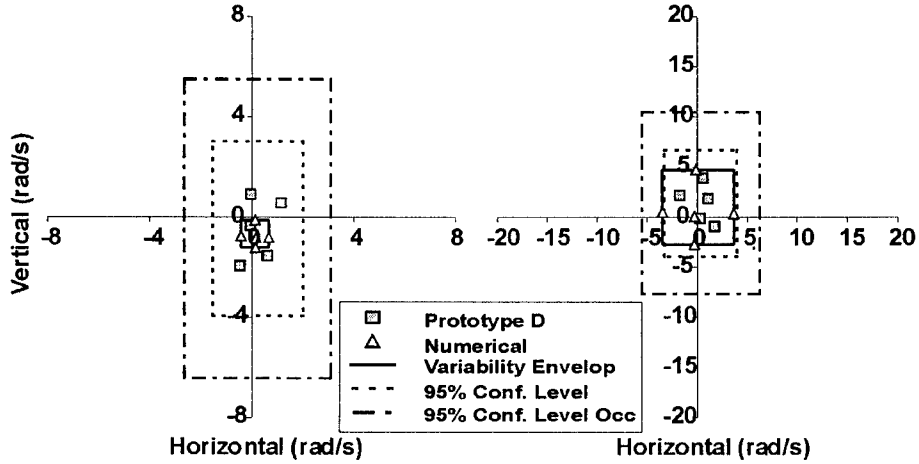

FIGURE 15. TRANSVERSE VELOCITY AND ANGULAR RATE COMPARISONS, RESPECTIVELY FOR PROJECTILE D.

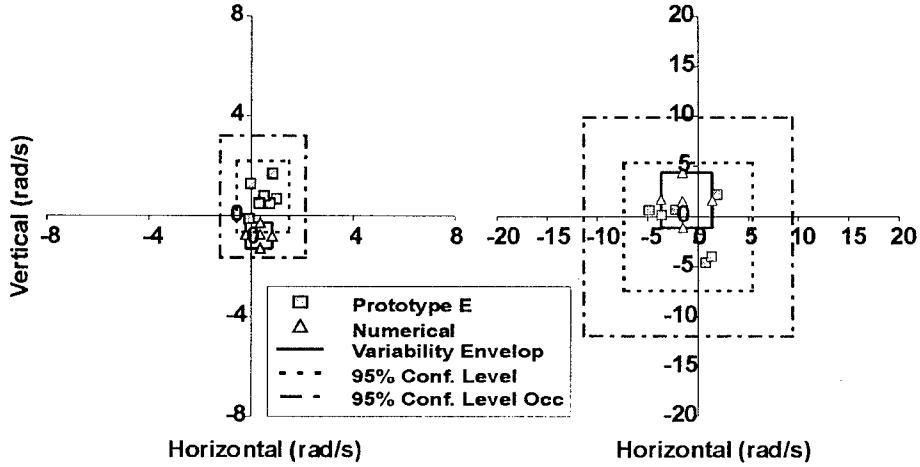

FIGURE 16. TRANSVERSE VELOCITY AND ANGULAR RATE COMPARISONS, RESPECTIVELY FOR PROJECTILE E.

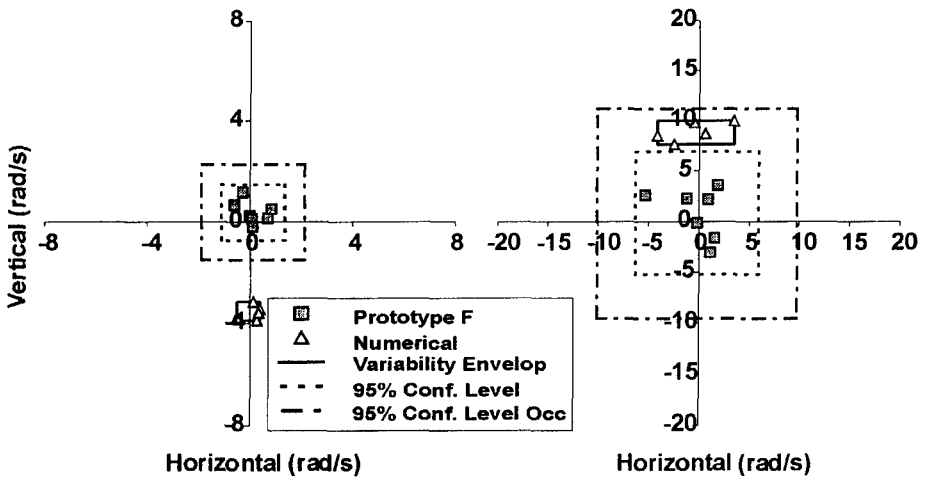

FIGURE 17. TRANSVERSE VELOCITY AND ANGULAR RATE COMPARISONS, RESPECTIVELY FOR PROJECTILE F.

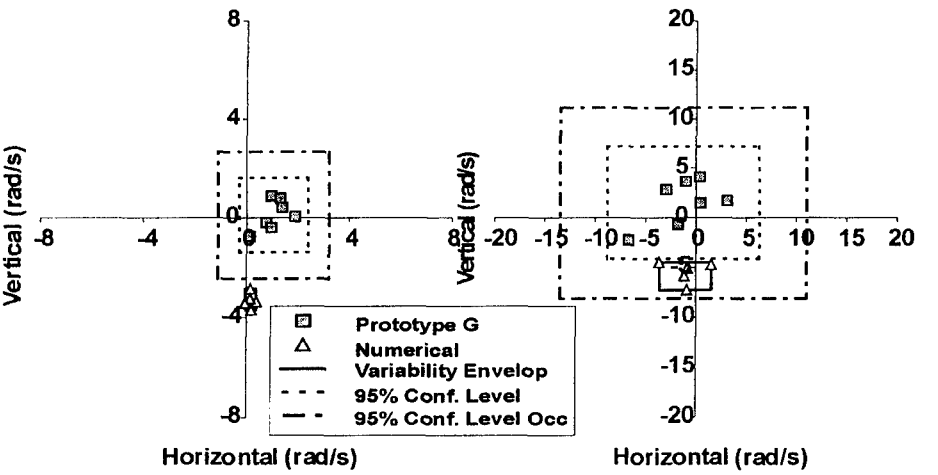

FIGURE 18. TRANSVERSE VELOCITY AND ANGULAR RATE COMPARISONS, RESPECTIVELY FOR PROJECTILE G.

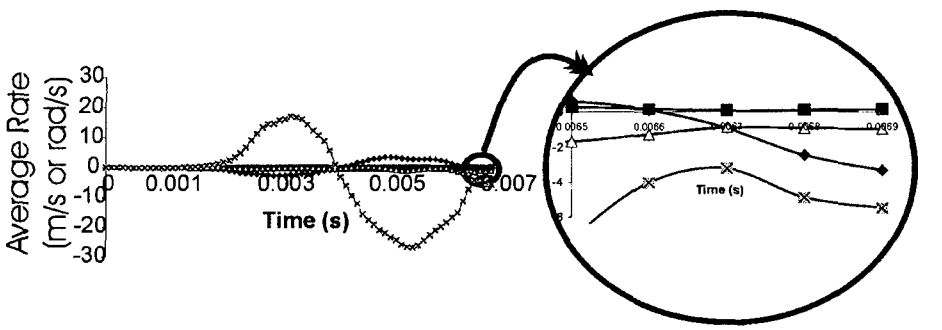

FIGURE 19. AVERAGE TRANSVERSE RATES AND ACCELERATIONS DURING LAUNCH FOR PROTOTYPE G

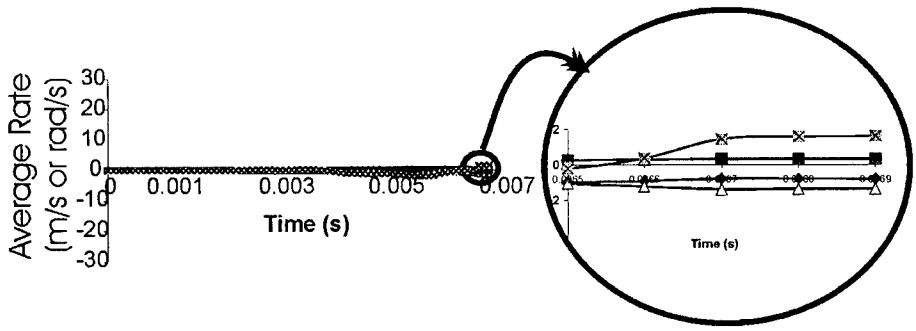

FIGURE 20. AVERAGE TRANSVERSE RATES AND ACCELERATIONS DURING LAUNCH FOR PROTOTYPE E.

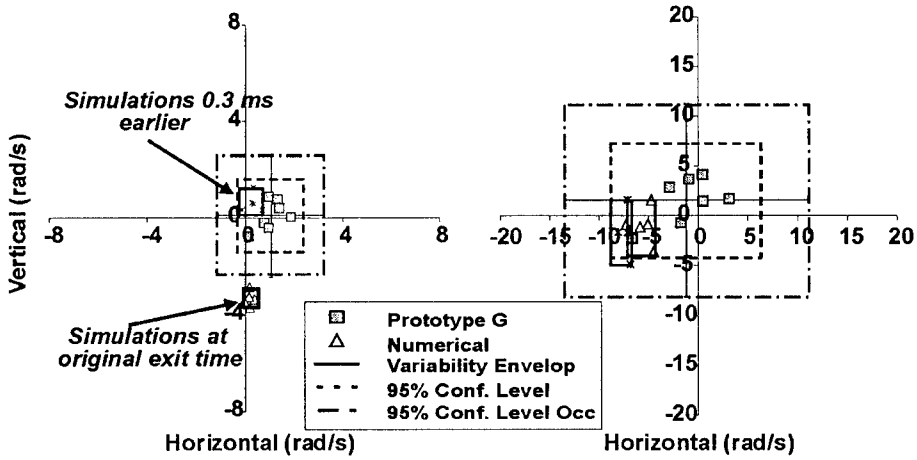

FIGURE 21. MULTIPLE TIME COMPARISONS FOR PROTOTYPE G.

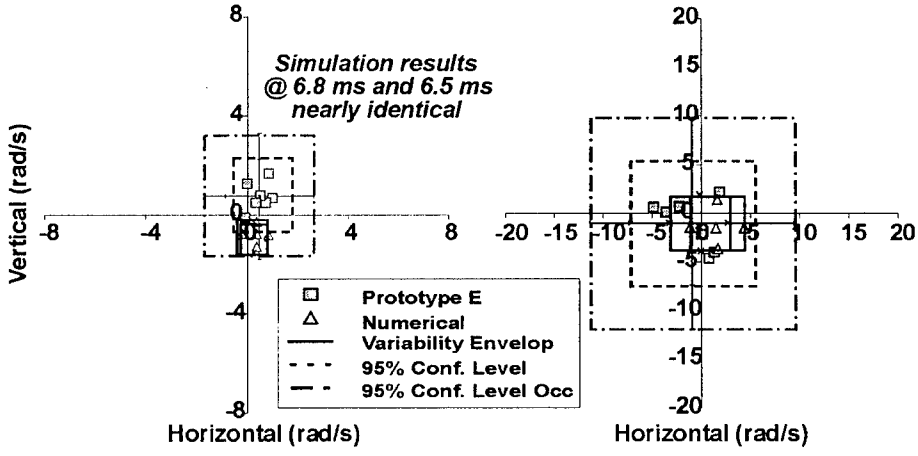

FIGURE 22. MULTIPLE TIME COMPARISONS FOR PROTOTYPE E.

6. CONCLUSION

It is quite clear that the computational capabilities to study the details of in-bore projectile motion are in hand. Predictions of the flight mechanics of the subprojectile are also tractable so that realistic predictions of fall of shot for complicated direct-fire projectiles are now feasible. We have started to couple this advanced modeling capability to the design of future generations of systems. From this we expect significant economic advantages to emerge along with reduced time

expenditures for development coupled with a direct method of reducing gun system and projectile contributions to accuracy.

The numerical methodology also permits new insight into the dynamical behavior of the projectile while undergoing in-bore acceleration. The derivation of dynamic performance envelopes should now allow the definition of realistic specifications for electronic modules, sensors, and sensitive mechanisms associated with advanced submunitions and maneuvering (smart) projectiles. With the maturation of these high-performance technologies, the projectile designer now finally has very powerful tools to rely on the design process; the challenge is to make them assessable and timely.

7. ACKNOWLEDGEMENTS

A study of this magnitude requires a coordinated effort and support from many people. The principal organizations are Project Manager for Tank and Medium-caliber Armament Systems (TMAS) program office, U.S. Tank Automotive and Armament Command (TACOM) Armament Research, Development, and Engineering Center (TACOM-ARDEC), Alliant Techsystem Inc, and General Dynamics Ordnance and Tactical Systems. Their leadership expertise and experience are invaluable. This study relied heavily on supercomputers supplied by DOD's High Performance Computing initiative (specifically by the Major Shared Resource Center at ARL).

8. REFERENCES

Anderson, R. D., and K. D. Fickie. "IBHVG2 - A User's Guide." BRL-TR-2829, U.S. Army Ballistic Research Laboratory, Aberdeen Proving Ground, MD, July 87.

Bornstein, J., and B. Haug, "Gun Dynamics Measurements for Tank Gun Systems." BRL-MR-3688, U.S. Army Ballistic Research Laboratory, Aberdeen Proving Ground, Maryland, May 88 .

Bornstein, J., I. Celmins, and P. Plostins, "Launch Dynamics of Fin-Stabilized Projectiles." AIAA Paper No. 89-3395, August 89.

Bornstein, J., D.S. Savick, D.H. Lyon, E.M. Schmidt, J. Kietzman, and D. Deaver, "Simulation of Tank Cannon Launch Dynamics." Proceedings of The Seventh U.S. Army Gun Dynamics Symposium, May 93 .

Bornstein, J., I. Celmins, P. Plostins, E. M. Schmidt, "Techniques for the Measurement of Tank Cannon Jump." BRL-MR-3715, US Army Ballistic Research Laboratory, Aberdeen Proving Ground, Maryland, December 88.

Bundy, M.L., "Thermal Distortion Protection by Candidate Metal and Composite Thermal Shrouds for 120-mm Tank Cannon." BRL-TR-2807, U. S. Army Ballistic Research Laboratory, Aberdeen Proving Ground, Maryland, June 87 .

Bundy, M.L., N. Gerber, and J.W. Bradley, "Thermal Distortion Due to Wall Thickness Variation and Uneven Cooling in an M256 120-mm Gun Barrel, U.S. Army Research Laboratory, Aberdeen Proving Ground, Maryland, September 93 .

Guidos, B. J. and G. R. Cooper. "The Effect of a Simple Lateral Impulse on Kinetic Energy Projectile in Flight." ARL-TR-2076, U.S. Army Research Laboratory, Aberdeen Proving Ground, Maryland, Dec 99.

Lyon, D.H., D.S. Savick, and E.M. Schmidt, "Comp. of Computed and Measured Jump of 120mm Cannon." AIAA Paper 91-2898, Jul 91.

Murphy, C.H., "Free Flight Motion of Symmetric Missiles." BRL-R-1216, U.S. Army Ballistic Research Laboratories, aberdeen Proving Ground, Maryland, July 63 .

Newill J.F., B.P. Burns, and S.A. Wilkerson, "Overview of Gun Dynamics Numerical Simulations." Technical Report in work, US Army Research Laboratory, Aberdeen Proving Ground, Maryland, July 98a.

Newill J.F., C. P. R. Hoppel, and W. H. Drysdale, "Comparison of Launch Mechanics and Dynamics from the M1A1 M256 Gun System for the M829A2 Kinetic Energy Long Rod Fin Stabilized Projectile Containing Different Penetrator Materials." Technical Report 1671, US Army Research Laboratory, Aberdeen Proving Ground, Maryland, April 98b.

Newill J.F., D. Webb, B. Guidos, C.P.R. Hoppel, and W.A. Drysdale, "Methodology for Formal Comparison of Experimental Ballistic Firing of Kinetic Energy Projectiles with Numerical Simulation." Technical Report in work, US Army Research Laboratory, Aberdeen Proving Ground, MD.

Newill J.F., S.A. Wilkerson, C.P.R. Hoppel, and W.H. Drysdale, "Numerical Simulation of Launch Interaction of Kinetic Energy Long Rod Fin-Stabilized Projectiles and M1A1 Abrams M256 Gun System with Comparison to Experimental Results." Classified Ballistics Symposium, Elgin Air Force Base, FL, May 11-14, 98c.

Newill, J.F., C.P.R. Hoppel, and W.H. Drysdale, "Comparison of Launch Mechanics and Dynamics from the M1A1 M256 Gun System for the M829A2 Kinetic Energy Long Rod Fin Stabilized Projectile Containing Different Penetrator Materials." ARL-TR-1671, U.S. Army Research Laboratory, Aberdeen Proving Ground, Maryland, April 98d.

Plostins, P., I. Celmins, and J. Bornstein, "The Effect of Sabot Front Borerider Stiffness on the Launch Dynamics of Fin-Stabilized Kinetic Energy Ammunition." AIAA Paper No. 90-0066, January 90.

Rabern D. A., "Axially Accelerated Saboted Rods Subjected to Lateral Forces." Contractor Report No. 671, US Army Ballistic Research Laboratory, Aberdeen Proving Ground, Maryland, August 91.

Rabern, D.A., "Axially Accelarated Saboted Rods Subjected to Lateral Forces." LA-11494-MS, Los Alamos National Laboratory, Los Alamos, New Mexico, March 89 .

Webb, D.W., "Optimal Partitioning of M829A1 Cartridges for the TGAD Jump Test." ARL-TR-55, U.S. Army Research Laboratory, Aberdeen Proving Ground, Maryland, June 99 .

Wilkerson S. A. and D. Hopkins, "Analysis of a Balanced Breech System for the M1A1 Main Gun System Using Finite Element Techniques." Technical Report 608, US Army Research Laboratory, Aberdeen Proving Ground, Maryland, November 94.

9. BIBLOGRAPHY

Burns B. P., "MC-AAAC In-Bore Projectile Technology." Technical Report ARBRL-TR-02364, US Ballistic Research Laboratory, Aberdeen Proving Ground, Maryland, September 81.

Burns B.P., D. L. Henry, C. D. McCall, and J. F. Newill, "Flexural Characteristic of the M829 Projectile Family." Technical Report 1201, US Army Research Laboratory, Aberdeen Proving Ground, Maryland, September 96

Held, B.J., and D.W. Webb, "Tank Cannon Accuracy Error Due to Inaccurate Measurement of Ammunition Temperature." ARL-MR-128, U.S. Army Research Laboratory, Aberdeen Proving Ground, Maryland, February 94 .

Held, B.J., and T.F. Erline, "Dynamics of the Balanced Breech System for the 120mm Tank Main Gun." BRL-TR-3186, U.S. Army Ballistic Research Laboratory, Aberdeen Proving Ground, Maryland, January 91 .

Held, B.J., D.W. Webb, and E.M. Schmidt "Temperture Dependent Jump of the 120 mm M256 Tank Cannon." BRL-MR-3927, U.S. Army Ballistic Research Laboratory, Aberdeen Proving Ground, Maryland, December 91 .

Hopkins D. A., "Predicting Dynamic Strain Amplification by Coupling a Finite Element Structural Analysis Code with and Interior Ballistic Code." Technical Report No. 3269, US Ballistic Research Laboratory, Aberdeen Proving Ground, MD, September 91.

Hoppel C.P.R., J.F. Newill, and W.H. Drysdale, "Design Optimization of Composite Sabots for Kinetic Energy Projectiles." Classified Ballistics Symposium, Eglin Air Force Base, FL, May 11-14, 98.

Kirkendall, R.D., "Physical Measurements of M829A1 Cartridges for an Accuracy Test." ARL-CR-243, U.S. Army Research Laboratory, Aberdeen Proving Ground, Maryland, September 95 .

Plostins, P., "Launch Dynamics of APFSDS Ammunition." BRL-TR-2595, U.S. Army Ballistic Research Laboratory, Aberdeen Proving Ground, Maryland, October 84 .

Schmidt, E. M., P. Plostins, and M. Bundy, "Flash Radiographic Diagnostics of Projectile Launch from Cannon." Proceedings of 84 Flash Radiography Symposium, E.A. Webster, Jr. And A.M. Kennedy, Eds., The American Society for Nondestructive Testing, 84.

Schmidt, E.M., and D. D. Shear, "Aerodynamic Interference during Sabot Discard." USABRL Report R-20, U.S. Army Ballistic Research Laboratory, Aberdeen Proving Ground, Maryland, September 77. (AD A50308)

Schmidt, E.M., J.A. Bornstein, P. Plostins, B. Haug, and T.L. Brousseau, "Jump from M1A1 Tank." BRL-TR-3144, U.S. Army Ballistic Research Laboratory, Aberdeen Proving Ground, Maryland, September 90 (CONFIDENTIAL).

Schmidt, E.M., P. Plostins, and M. Bundy, "Flash Radiographic Diagnostics of Projectile Launch from Cannon." Proc. of 84 Flash Radiography Symposium, E.A. Webster, Jr. And A.M. Kennedy, Eds., The American Society for Nondestructive Testing, 84 .

Siegleman, D., J. Wang, and P. Crimi, "Computation of Sabot Discard." U.S. Army Ballistic Research Laboratory, Aberdeen Proving Ground, Maryland, BRL Contract Report ARBRL-CR-505, February 83 .

Tzeng J. T. and D. A. Hopkins, "Dynamic Response of Composite Gun Tubes Subjected to a Moving Internal Pressure." Technical Report No. 889, US Ballistic Research Laboratory, Aberdeen Proving Ground, Maryland, October 95.

Wilkerson S. A., M. Berman, and M TingLi, "A Modal Survey of the M1A1 Main Weapon System." Proceedings of the 7th U.S. Army Symposium on Gun Dynamics, New Port RI, May 93.

Zucrow, M.J., and D. Hoffman, Gas Dynamics, John Wiley and Sons, Inc. 76 .